Integration of graphene into nanoelectronic devices: insights from atomistic simulations

M. García-Mota[*], D. J. Oroya[*], E. Artacho[**], X. Cartoixà[***] and J. J. Palacios[****]

[*]Simune Atomistic Simulations, Tolosa Hiribidea 76, 20018
Donostia-San Sebastián, Spain, m.garcia@simune.eu
[**]CIC Nanogune and DIPC, Tolosa Hiribidea 76, 20018 Donostia-San Sebastián, Spain and Basque Foundation for Science Ikerbasque, Bilbao, Spain. 3 Theory of Condensed Matter, Cavendish Laboratory, University of Cambridge, J.J. Thomson Avenue,
Cambridge CB3 OHE, United Kingdom, e.artacho@nanogune.eu
[***]Departament d'Enginyeria Electrònica,
Universitat Autònoma de Barcelona, 08193 Bellaterra, Catalonia, Spain, Xavier.Cartoixa@uab.cat
[****]Departamento de Física de la Materia Condensada, Instituto Nicolás Cabrera (INC), and Condensed Matter Physics Center (IFIMAC), Universidad Autónoma de Madrid, Cantoblanco, 28049 Madrid, Spain, juanjose.palacios@uam.es

ABSTRACT

The preparation of high quality graphene as host material is pivotal for further device applications. As such, a deep knowledge on the electronic and transport properties of graphene derivatives is critical to successful integration of graphene into future nanoelectronic devices. In this work, the influence of gas adsorption on the electrical characteristics of graphene, and the effect of intrinsic defects on graphene electronic properties are explored by performing Density Functional Theory (DFT) calculations. Contact resistance between graphene and metal electrodes is also critical for obtaining efficient graphene devices. The contact resistance between graphene and various metals in different geometries is characterized by performing first-principles quantum transport calculations.

Keywords: graphene, transport, molecular doping, mechanical strain, grain boundaries

1 INTRODUCCTION

Graphene has material's unique electronic properties. The unusual properties of carriers in graphene are a consequence of the gapless and approximately linear electron dispersion at the vicinity of the Fermi level at two inequivalent points of the Brillouin zone. In the low-energy limit, the quasiparticles in these systems are described in terms of massless chiral relativistic fermions governed by the Dirac equation. The called massless Dirac fermions behave as a two-dimensional electron gas with ballistic transport behavior on the micrometer scale [1]. Contaminants such as water and oxygen molecules may affect transport properties of graphene by binding at its surface. Previous theoretical calculations have addresed the strength of the molecular doping of H [2], O_2, NO [3, 4], H_2O, NH_3, CO and NO_2 [4] molecules adsorbed on pristine graphene. Graphene can at present be grown at large quantities only by the chemical vapor deposition method, which produces polycrystalline samples. The electronic and mechanical properties of polycrystalline materials are expected to be affected by the presence of intrinsic defects and grain boundaries (GB) [5]. In this work DFT calculations are performed to describe the uptake of CO_2, O_2 and N_2 by graphene. The effect of the presence of intrinsic defects and grain boundaries on graphene electronic properties is also addressed.

One of the technological hurdles that must be overcome in order to harness the possibilities of graphene [1, 6] and two-dimensional materials (2DMs) [7] for electronics is achieving a low enough contact resistance (Rc) so that the high-frequency performance is not compromised [8, 9]. For graphene, it is often quoted that an Rc value lower than 100 Ω· μm is desirable, while larger values are thought to be a limiting factor on the graphene field effect transistor performance [10]. Recent experiments have achieved this landmark value with a top contact geometry [11]. We use atomic simulations to examine the influence of different contact geometries and metals on the contact resistance to Graphene, and to determine the most efficient system.

2 COMPUTATIONAL DETAILS

All the Density Functional Theory (DFT) calculations have been carried out within the generalized gradient approximation of Perdew–Burke–Ernzerhof (GGA-PBE) approximation implemented in the SIESTA code [12]. It is expected GGA to overestimate the distance between

adsorbate and the graphene surface, and consequently underestimate the binding energy. As a consequence, the advantage of GGA over the local density approximation (LDA) in this work is that the GGA will not lead to a strong bonding of the molecules as in LDA. So, if the molecules bind in GGA, they will definitely bind in a real system (and in LDA) too. The wave functions for the valence electrons are represented by a linear combination of pseudoatomic numerical orbitals using a double-ζ basis. The spacing of the real space grid used to calculate the Hartree and exchange and correlation contribution to the total energy and Hamiltonian was 400 Ry. Periodic boundary conditions were used, and the inter-graphene distance was kept to a minimum of 20 Å to avoid interactions between adjacent graphene layers. Sampling of the 2D Brillouin zone was carried out with a 3 × 3 × 1 Monkhorst−Pack grid, which is tested to give converged results for all the properties we calculate. The density of states (DOS) was obtained using a 15 × 15 × 1 grid, and a Gaussian smearing of 0.14 eV.

In order to caracherize the contact resistance between graphene and various metals, a geometry directly connected with experimental measurements [13] is considered; a single top contact geometry with a finite contact overlap L and infinite contact width for Al, and Pd injecting electrodes [modeled by a 6-layered structure in the (111) direction], see Figure 1. The metals are under the necessary hydrostatic strain so that their lattices match that of pristine graphene. The graphene atoms are then allowed to relax until the force felt by each of them is lower than 0.04 eV/Å. The exchange-correlation functional and basis-set used are the same as in the previous calculations (PBE and double-ζ basis). The TranSiesta code [14], which implements the NEGF formalism in systems with periodic boundary conditions perpendicular to the current, is used to obtain the zero-bias conductance (per unit of transverse length) after averaging the transmission coecients over 3056 kll-points.

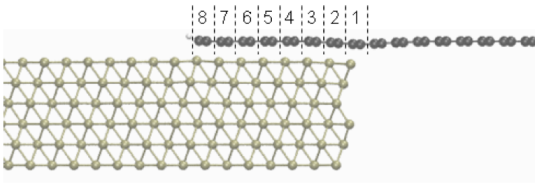

Figure 1 Structurally relaxed Pd(111)/graphene top contact, with a finite overlap (side view). Numbers indicate the amount of C atom pairs overlapping the Pd(111) contact.

3 RESULTS

3.1 Uptake of gases by graphene

We explore the gas uptake ability of graphene and the graphene's electronic properties after gas adsorption. We consider adsorption of those gases expected to be present at ambient conditions, such as CO_2, O_2 and N_2. First, the optimal adsorption position and orientation of each molecule on the graphene surface is determined, see Figure 2 , and the adsorption energies (E_{ads}) is calculated.

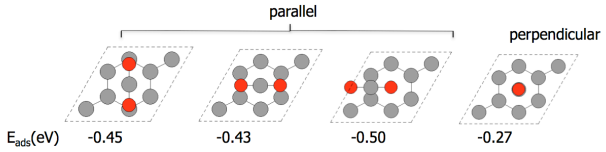

Figure 2 Schematic representation of the different configurations considered for CO_2 adsorption on graphene surface. Grey atoms refer to C, red to O. The calculated adsorption energies (E_{ads}) are indicated for each configuration.

E_{ads} is calculated as the energy of the fully relaxed graphene sheet with the molecule adsorbed on it ($E_{X\text{-}graphene}$) minus the energy of the isolated graphene sheet ($E_{graphene}$) and isolated molecule (E_X), with X CO_2, O_2 or N_2.

$$E_{ads}=E_{X\text{-}graphene}-E_X - E_{graphene} \quad (1)$$

E_{ads} of CO_2, O_2 or N_2 on graphene surface, at the optimal adsorption position and orientation of each molecule, is calculated to be -0.41, 0.31, -0.34 respectively. These low values indicate that the considered molecules are physisorbed in graphene. Further DFT calculations within the van der Waals functional should be thus performed in order to obtain an accurate description of the molecular physisorption. To check the consistency of the calculations, the graphene supercell size is varied and test calculations of gas-adsorbed graphene are performed.

Molecular doping, i.e., charge transfer between the molecules and the graphene surface, can be discussed in light of the Density of States (DOS) and the molecular orbitals of the adsorbates. In the case of chemisorption, the charge transfer from the gas molecule to the graphene surfaxe, or viceversa would be a key factor affecting the transport properties. However, as expected for phisisorbed molecules, the calculated DOS does not present distint changes near the Fermi level compared with pristine graphene for any of the adsorbates considered here, see Figure 3. Therefore, it is not expected a dramatic conductance change of the pristine graphene upon adsorption of the considered molecules, CO_2, O_2 or N_2 .

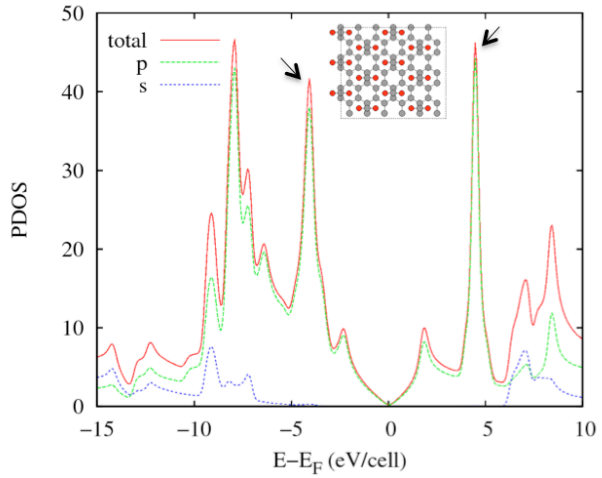

Figure 3 Projected density of states (PDOS) of graphene covered by CO_2. The arrows indicate the main peaks introduced by CO_2.

3.2 Grain boundaries

Graphene can at present be grown at large quantities only by the chemical vapor deposition method, which produces polycrystalline samples. The electronic and mechanical properties of polycrystalline materials are defined by important intrinsic defects of various kind: topological defects, kinks, vacancies and impurities [15]. In this work, DFT calculations are performed to describe the effect of the presence of intrinsic defects and grain boundaries on the uptake of gases (CO_2, O_2 or N_2) by graphene. One of the simplest topological defects, a Stone – Wales defect, consisting of two pentagon – heptagon pairs, is considered. The structural model proposed by Simonis *et al.*, who observed a large-angle tilt boundary on the surface of HOPG, on STM experiments is used to simulate a grain boundary [16], see Figure 4.

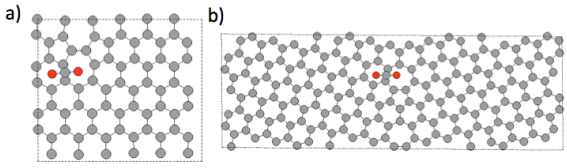

Figure 4 Schematic representation of one of the adsorption sites considered to simulate CO_2 adsorption on graphene with the presence of a) a Stone – Wales defect, b) GB consisting of a periodic structure that can be described as a regular succession of pentagon-heptagon pairs. Grey atoms refer to C, red to O.

Calculated adsorption energies and DOS analysis indicate that the picture of molecular physisorption (CO_2, O_2 or N_2) is not substantially altered neither by the presence of the Stone–Wales pairs, nor by the presence of the considered GB.

3.3 Contact resistance between metals and graphene

Contact resistance between graphene and metal electrodes is critical for obtaining efficient graphene devices. In this work, the contact resistance between graphene and various metals in different geometries is characterized by performing first-principles quantum transport calculations. Pd and Al tips are chosen as examples of metals with strong and weak coupling to graphene, respectively. In the case of Pd one or two strong metal-C bonds are found enough to saturate the current carrying capability of a row of C atoms in graphene, and a one/two- bond edge or top contact provides transmission values at par with wider overlap top contacts, see Figure 5 Width-normalized conductance (G in units of $G_0 = e^2/h$ per transverse unit length a_t) around the Dirac point (E = 0) of the suspended graphene for (a) Pd and (b) Al electrodes and various contact lengths [given in units of the surface lattice constant, as indicated in Figure 1]. The dashed line indicates the L=2-8 mean, and the blue shade corresponds to ± σ (σ being the standard deviation). A free (pristine) graphene sheet shows the upper limit in conductance.

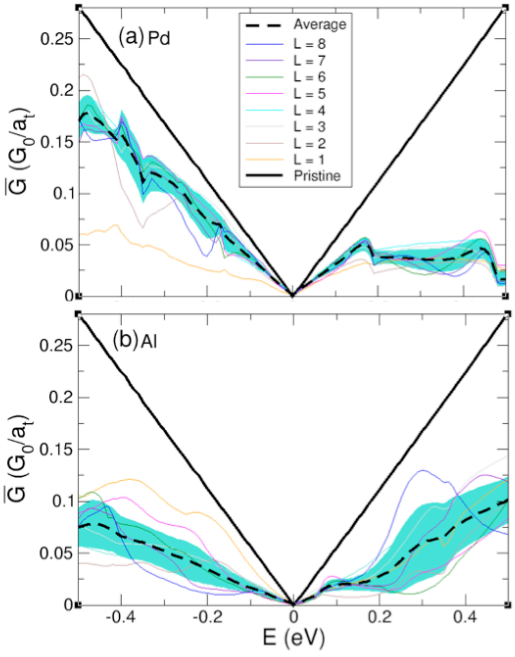

Figure 5 Width-normalized conductance (G in units of $G_0 = e^2/h$ per transverse unit length a_t) around the Dirac point (E = 0) of the suspended graphene for (a) Pd and (b) Al electrodes and various contact lengths [given in units of the surface lattice constant, as indicated in Figure 1]. The

dashed line indicates the L=2-8 mean, and the blue shade corresponds to ± σ (σ being the standard deviation). A free (pristine) graphene sheet shows the upper limit in conductance.

REFERENCES

[1] Castro Neto, A., Guinea, F., Peres, N., Novoselov, K., & Geim, A. (2009). Rev. Mod. Phys. 81, 109–162.

[2] Boukhvalov, D. W., & Son, Y. W. (2012). ChemPhysChem, 13, 1463–1469.

[3] Pramanik, A., & Kang, H. S. (2011). J. Phys. Chem. C, 115, 10971–10978.

[4] Leenaerts, O., Partoens, B., & Peeters, F. M. (2008). Phys. Rev. B, 77, 125416.

[5] a) Yazyev, O. V., and Louie, S. G., (2010) Phys. Rev. B 81 1; b) Mesaros A., Papanikolaou, S., Flipse, C. F., Sadri, D. and Zaanen (2010). J. Phys. Rev. B, 82, 1. c) Nemes-Incze, P. Vancsó, P. Osváth, Z. et. al. Carbon, (2013). 64, 178. d) Li Z.-L, Li Z-M., H.-Y. et. al. (2014). Nanoscale, 6, 4309

[6] Novoselov, K. S., Geim, A. K., Morozov, S. V, Jiang, D., Zhang, Y., Dubonos, S. V et al. (2004). Science (New York, N.Y.), 306, 666–9.

[7] S. Z. Butler, S. M. Hollen, L. Cao, Y. Cui, J. A. Gupta, H. R. Gutiérrez, T. F. Heinz, S. S. Hong, J. Huang, A. F. Ismach, E. Johnston-Halperin, M. Kuno, V. V. Plashnitsa, R. D. Robinson, R. S. Ruo, S. Salahuddin, J. Shan, L. Shi, M. G. Spencer, M. Terrones, W. Windl, and J. E. Goldberger, (2013) ACS Nano 7, 2898.

[8] J. Moon, D.K. Gaskill, P. Campbell, and P. Asbeck, (2011). IEEE MTT-S International Microwave Symposium.

[9] Fiori, G., Bonaccorso, F., Iannaccone, G., Palacios, T., Neumaier, D., Seabaugh, A., Colombo, L. (2014) Nature Nanotechnol., 9, 768–779.

[10] Venugopal, A., Colombo, L., & Vogel, E. M. (2010). Appl. Phys. Lett., 96, 013512–1–3.

[11] J. S. Moon, M. Antclie, H. C. Seo, D. Curtis, S. Lin, A. Schmitz, I. Milosavljevic, A. A. Kiselev, R. S. Ross, D. K. Gaskill, P. M. Campbell, R. C. Fitch, K.-M. Lee, and P. Asbeck, (2012). Appl. Phys. Lett. 100, 203512

[12] a) P. Ordejon, E. Artacho, and J. M. Soler, Phys. Rev. B 53, (1996) R10441. b) J. M. Soler, E. Artacho, et al., J. Phys.: Condens. Matter 14, (2002) 2745

[13] Nagashio, K., Nishimura, T., Kita, K., & Toriumi, A. (2010). App. Phys. Lett., 97(14).

[14] M. Brandbyge, J.-L. Mozos, P. Ordejón, J. Taylor, and K. Stokbro, (2002). Phys. Rev. B 65, 165401

[15] a) Z.-L, Li, Z-M. Li, H.-Y.et al Nanoscale, 6, (2014) 4309 ; b) O. V. Yazyev, and S. G. Louie (2010). Phys. Rev. B 81 1; c) A. Mesaros, S. Papanikolaou, C. F. Flipse, D. Sadri, and J. Zaanen (2010), Phys. Rev. B, 82, 1. d) J. Kotakoski, and J.C. Meyer (2012) Phys. Rev. B , 85 1. e) P. Nemes-Incze, P. Vancsó, Z. Osváth, et al (2013) Carbon, 64, 178.

[16] P. Simonis, C. Goffaux, P. Thiry, L. Biro, P. Lambin, and V. Meunier, (2002). Surf. Sci., 511, 319–322.